Synthesis, vibrational, thermal, topological, electronic, electrochemical stability and DFT studies of new DABCO based ionic liquids

Behzad Khalili, Boumediene Haddad, Khatereh Ghauri, Mohammad Rizehbandi, Bekhaled Fetouhi, Touil Aya Khadidja, Annalisa Paolone, Didier Villemin, Mustapha Rahmouni, Serge Bresson

Synthesis, vibrational, thermal, topological, electronic, electrochemical stability and DFT studies of new DABCO based ionic liquids.

Behzad Khalili[1], Boumediene Haddad *[,2,3], Khatereh Ghauri[1], Mohammad Rizehbandi[1],Bekhaled Fetouhi[4,5], Touil Aya Khadidja[2], Annalisa Paolone[6], Didier Villemin[3], Mustapha Rahmouni[5], Serge Bresson[7]

[1] Department of Chemistry, Faculty of Sciences, University of Guilan, Rasht, Iran
[2] Department of Chemistry, Faculty of Sciences, University of Saida - Dr.Moulay-Tahar, 20000, Algeria.
[3]LCMT, ENSICAEN, UMR 6507 CNRS, University of Caen, 6 bd Ml Juin, 14050 Caen, France
[4]Faculty of Natural and Life Sciences, University of Tiaret, BP78 ZaarouraTiaret 14000, Algeria.
[5] Synthesis and Catalysis Laboratory LSCT, Tiaret University, Tiaret, Algeria.
[6]CNR-ISC, U.O.S. La Sapienza, Piazzale A. Moro 5, 00185 Roma, Italy
[7] UP Transformations & Agro-Ressources, Institut Polytechnique UniLaSalle, SFR Condorcet 3417, BP 30313, F-60026 Beauvais, France.

*Corresponding author: Tel.: +213676802567
E-mail :haddadboumediene@yahoo.com (HADDAD Boumediene).

Abstract

The design of new ILs with different anions could provide interesting physico-chemical properties and, for these reasons, the knowledge about the synthesis, the thermal, vibrational, topological, electronic, electrochemical properties and interaction between coupled selected cation-anion in these ILs are important subjects. Therefore, the understanding about these properties of these compounds is an important subject of study. In this work, we studied three ionic liquids based on the 1-decyl-1,4-diazabicyclo [2.2.2] octane, DABCO-cation, where the corresponding anions were $[Br]^-$, $[PF_6]^-$, and $[N(SO_2CF_3)_2]^-$. The syntheses of these bicyclic DABCO ILs are based on an alkylation reaction of 1,4-diazabicyclo [2.2.2] octane and 1-bromodecane followed by anion exchange. The obtained ILs are characterized by ^1H, ^{13}C, ^{19}F and ^{31}P-NMR spectroscopy. Vibrational spectroscopy studies are conducted by infrared (FTIR/ATR) and Raman spectroscopy in the wavenumber range 600-4000 cm^{-1} and 45-3500 cm^{-1}, respectively. Furthermore, the thermal stabilities were investigated using the thermogravimetric analysis (TGA) method. Results indicate that the thermal stability follow the order $[C_{10}DABCO][Br]<[C_{10}DABCO][PF_6]<[C_{10}DABCO][N(SO_2CF_3)_2]$. Additionally, the structural parameters, electrostatic potential (ESP) maps, interaction energies, non-covalent interaction (NCI), atoms in molecule (AIM) analysis, natural bond orbital (NBO), frontier molecular orbital (FMO) analysis and Electrochemical window (ECW) are studied and analyzed by means of DFT calculations at the M06-2X-GD3/AUG–cc–pVDZ level of theory.

KEYWORDS: DABCO; ionic liquid; NMR; IR/Raman spectroscopy; ESP; NCI ; DFT calculations.

1. Introduction

The concept of “green chemistry” has led organic chemists to rethink their synthesis methods. Catalysis, microwave activation, replacement of organic solvents are developments towards processes with limited waste production [1]. In the context of eco-compatible chemistry, the use of ionic liquids (IL) as new reaction media seems to be a good alternative to pre-existing methods [2]. Ionic liquids have a low vapor pressure, which facilitates their recycling [3]. Their particularly interesting and unique physicochemical properties make them attractive candidates for various applications [4], particularly in organic synthesis and catalysis [5,6]. Ionic liquids based on DABCO (1,4-diazabicyclo [2.2.2] octane) known also as triethylenediamine, due to their bicyclic “cage” structure, show weak alkalinity and medium-hindrance [7], that make it a useful organo-catalyst in the synthesis of many heterocyclic [8]. Furthermore this family of ILs is compatible with many organic reactions and widely utilized in organic synthesis reactions as a catalyst and reagent, with the advantage of recovering the latter at the end of the reaction.

Most researchers have been focusing their attention on the synthesis of new DABCO based ionic liquids [9-10] and their properties for device applications. Wykes and MacNeil indicated that the presence of the tertiary nitrogen in the cation which, although significantly diminished in basicity relative to DABCO [11]. In the area of green chemistry; DABCO based ionic liquids have been the subjects the study of Faisal et al [12]; these authors have been developed a series of deep eutectic solvents based on DABCO-derived quaternary ammonium salts and applied them as promising reaction medium in gaining access to terpyridines. Moreover, Mondal et al. evaluated the performance of DABCO-based acidic-ionic-liquid-supported ZnO nanoparticles and examined their catalytic activity in the synthesis of N-aryl poly-substituted pyrrole derivatives [13]. Ying et al. developed an array of DABCO based ionic liquids and used as an efficient and recyclable catalysts for the aza-Michael addition of various amines and a wide range of α, β-unsaturated amides under solvent-free conditions [14]. In addition, Zhang and his group [15] demonstrated that DABCO-based ionic liquid $[C_8DABCO][N(SO_2CF_3)_2]$ was a suitable solvent for the extraction of Rh(III) from high-concentration hydrochloric acid medium. Ishtiaq et al. [16] synthesized DABCO-C_5-F and DABCO-C_7-F and investigated their efficiency for the synthesis of indoles and 1,4-dihydropyridines.

The correlation of the structure and properties of this family of ionic liquids is essential for make the selection of ILs easier for a particular application. In view of this, a detailed vibrational spectroscopic analysis and quantum-chemical calculation were performed to explore the interionic interactions in C_8DABCO cation and hexafluorophosphate anion-based ILs [17]. To date, only few experimental studies have been dedicated to illustrate the vibrational mode assignments of this bicyclic IL. Lauw et al. [18] have reviewed and discussed the structure of 1-ethyl-1,4-diazabicyclo [2.2.2] octanium bis(trifluoromethylsulfonyl)imide ($[C_2DABCO][N(SO_2CF_3)_2]$) and bromide precursor by single crystal X-ray diffraction, thermal study and Raman spectroscopy. Their studies show that the stronger electrostatic interaction between 1-ethyl-1,4-diazabicyclo [2.2.2] octanium and bromide, which is a smaller anion with a less shielded and more localized charge than bis(trifluoromethylsulfonyl)imide, and moreover has a higher symmetry compared to $[N(SO_2CF_3)_2]^-$, which has two low energy transoid and cisoid conformations. These two factors increase the relative packing density and efficiency of $[C_2DABCO][Br]$ in the crystal lattice. Recently and with the same objective, we have investigated by means of combined experimental and theoretical approaches, the structure and vibrational properties 1-octyl-1,4-diazabicyclo [2.2.2] octan-1-ium [C_8DABCO] with three types of counter anions i.e : bromide, hexafluorophosphate and bis-(trifluoromethylsulfonyl)imide by spectroscopic methods, such as nuclear magnetic resonance (^{1}H, ^{13}C, ^{19}F and, ^{31}P-NMR), Fourier transform infrared (FT-IR) and Raman spectroscopy [7, 17, 19].

Recently the use of quantum chemical computations before doing any experimental effort for synthesis and properties exploration of the new compounds is obtaining large consideration. Density functional theory (DFT) is a reliable and widely used tool to obtain information about the energetics, structure, transition states, and reaction pathways at relatively low computational cost with a high accuracy [20-29]. The synthesis and studies of ILs based on DABCO compared to other ILs are les spread, as literature review revealed. Also, the results indicated the cation-anion interactions play an important role on the structural, thermal, electronic, topological and vibrational properties of 1-octyl-1,4-diazabicyclo [2.2.2] octan-1-ium ILs [18, 19, 30] . In continuation of our interest in new structure of ionic liquids, as to the best of our knowledge no structural or electronic or vibrational data on 1-decyl-1,4-diazabicyclo [2.2.2] octan-1-ium [C_{10}DABCO] has been published, in present paper, the structure and some of the properties of some ILs with the $[C_{10}DABCO]^+$ cation coupled with the bromide ($[Br]^-$), hexafluorophosphate ($[PF_6]^-$) and bis-(trifluoromethylsulfonyl) imide

($[N(SO_2CF_3)_2]^-$) anions are studied and analyzed combining the ^{1}H-, ^{13}C-, ^{19}F-NMR, infrared and Raman spectra with DFT calculations at M06-2X-GD3/AUG–cc–pVDZ level of theory. Also, the experimental and thermal properties of these new ionic liquids were evaluated together with the calculations of their structural, vibrational, topological, electronic properties and electrochemical stability in the gas phase and acetonitrile solvent.

1. Experimental

2.1. Materials and methods

All the chemicals and reagents used in this work had analytical grades and were not purified before being utilized. 1,4-diazabicyclo [2.2.2] octane (>99%), 1-bromodecane (98%), potassium hexafluorophosphate ($[K]^+[PF_6]^-$), lithium bis(trifluoromethanesulfonyl)imide $[Li]^+[N(SO_2CF_3)_2]^-$, ethyl acetate, diethyl ether, were purchased from Fluka and used as received. The employed water (Deionized H_2O) was obtained with a Millipore ion-exchange resin deionizer (Merck KGaA, Darmstadt, Germany).

In the first step by using alkylation reaction the 1-decyl-1,4-diazabicyclo [2.2.2] octane bromide [C_{10}DABCO][Br] was synthesized via a previously reported method. Both ionic liquids [C_{10}DABCO][PF_6] and [C_{10}DABCO][$N(SO_2CF_3)_2$] were prepared as reported in our previous works [17, 19], and were characterized by means of ^{1}H, ^{13}C and ^{19}F-NMR infrared (IR) and Raman spectroscopy. The NMR analysis includes^{1}H-NMR (500 MHz), ^{13}C-NMR (125.75 MHz) ^{19}F-NMR (470.62 MHz) and ^{31}P-NMR (202.47 MHz) spectra that were recorded in DMSO-d_6 solution by using a Bruker-Neo 600MHz spectrometer.The chemical shifts were referenced to TMS as external standard. In the wavenumber range 45-4000 cm^{-1}, the FT-Raman spectra of three ILs were acquired with a resolution of 1 cm^{-1}, adding 128 scans at room temperature by a Vertex 70-RAM II Bruker FT-Raman spectrometer. Additionally, between 4000 and 600 cm^{-1}, the FT-IR spectra of [C_{10}DABCO][Br], [C_{10}DABCO][PF_6] and [C_{10}DABCO][$N(SO_2CF_3)_2$] were recorded with a spectral resolution of 1 cm^{-1} adding 64 scans on a Bruker Vertex II-70RAM Spectrometer (Bruker Analytical, 7Slough, United Kingdom).

The thermal stability of three investigated ILs was examined by thermogravimetric analysis (TGA) in the temperature range [25 to 700 °C]; the measurements were collected by means of a Setaram Setsys Evolution 1200 TGA system in an inert helium flux of 60 mL/min.

In the present study, the three DABCO ionic liquids are synthesized through an alkylation reaction of of1,4-diazabicyclo [2.2.2] octane, as displayed in Scheme 1. Briefly, a mixture of

equimolar 1,4-diazabicyclo [2.2.2] octane (10g, 89.1 mmol) and 1-bromodecane (19.70g, 90.1 mmol), mixed in AcOEt (125 ml) at room temperature for 24 hours was prepared. Rotatory evaporation at 40 °C with reduced pressure was utilized to eliminate the solvent and the obtained light yellow solid was washed with diethyl ether (100 mL) to yield the 1-decyl-1,4-diazabicyclo [2.2.2] octan-1-ium bromide [C_{10}DABCO][Br]. The recovered mass of this product is 27.05g.

The [C_{10}DABCO][PF_6] and [C_{10}DABCO][$N(SO_2CF_3)_2$] were synthesized through a simple anion exchange reactions as shown in Scheme 1. A solution of 1.66 g of potassium hexafluorophosphate [K][PF_6] in 10 mL of distilled water and a solution of 0.3 g of 1-decyl-1,4-diazabicyclo [2.2.2] octan-1-ium Bromide [C_{10}DABCO][Br] in 10 mL of distilled water were mixed in a flask with stirring for 2 hour at room temperature.

At the same manner, a solution of 2.58 g of lithium bis(trifluoromethanesulfonyl)imide $[Li]^+[N(SO_2CF_3)_2]^-$ in 10 mL of distilled water and a solution of 0.3 g of 1-decyl-1,4-diazabicyclo [2.2.2] octan-1-ium Bromide [$C_{10}DABCO^+$][Br^-] in 10 mL of distilled water were mixed in a flask with stirring for 2 hour at room temperature.After isolation of [C_{10}DABCO][PF_6] or [C_{10}DABCO][$N(SO_2CF_3)_2$] by centrifugation for 60 s, the obtained [C_{10}DABCO][PF_6] was a white solid at room temperature, while the [C_{10}DABCO][$N(SO_2CF_3)_2$] was recovered as a colorless liquid.

In order to obtain high purity, the three obtained DABCOILs were further dried in a high-vacuum line ($p<10^{-5}$ bar) for 3 days in phosphorus pentoxide (P_2O_5). The water content in [C_{10}DABCO][Br], [C_{10}DABCO][PF_6] and [$C_{10}DABCO^+$][$N(SO_2CF_3)_2$] was ~ 481, 374 and 562 ppm, respectively; these measures were carried out by coulometric Karl Fischer titration, performed by a Metrohm 831.

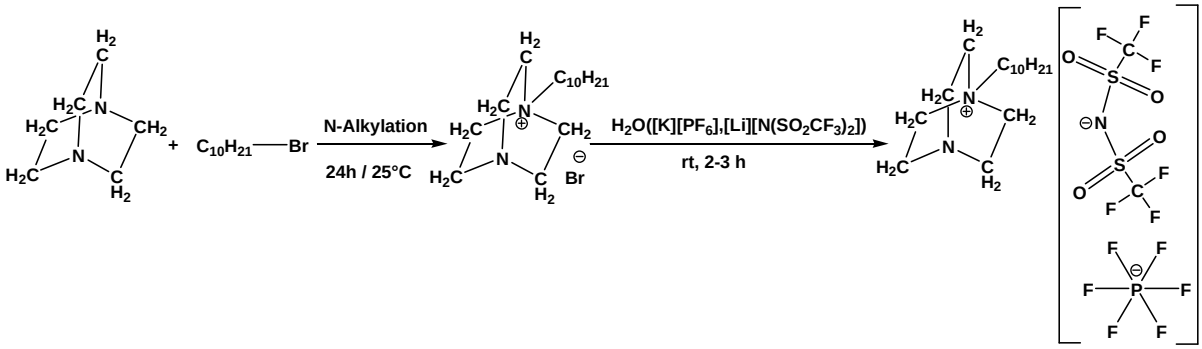

Scheme 1. Schematic representation of the synthesis route of [C_{10}DABCO][X](with X = $[Br]^-$,$[N(SO_2CF_3)_2]^-$ and $[PF_6]^-$).

Theoretical Calculations

1. Computational analysis

Density functional theory (DFT) calculations were used for the structural optimization of all investigated compounds including $[C_{10}DABCO]^+$ cation, $[Br]^-$, $[PF_6]^-$ and $[N(SO_2CF_3)_2]^-$ anions and all the ILs which are formed by combination of any of anion separately with the DABCO based cation. The calculations were performed at M06-2X-GD3/AUG–cc–pVDZ [31] level of theory in gas phase using Gaussian 09 software [32-34]. At the same level of theory, frequency calculations were performed on the optimized structures to make sure the structures are true minima and to characterize zero-point vibrational energy (ZPVE) as well as thermochemical quantities. Additionally, electrostatic potential (ESP) maps were evaluated to find the active sites of the cation and anions [35]. The NBO analysis was carried out using version 3.1 of NBO package and topological properties of electron charge density were also investigated by the AIM2000 program package at M06e2X-GD3/AUG–cc–pVDZ level of theory. The electrochemical stability of the ionic liquids was theoretically evaluated by the electrochemical window width (ECW).ECW of the ILs was calculated using COSMO-RS method at BVP86/TZVP level in the acetonitrile solvent at 298 K. The frontier molecular orbitals (FMO), FMO energy diagrams and quantum molecular descriptors of optimized structure of the ILs were investigated at M06-2X-GD3/AUG–cc–pVDZ level of theory.

3. RESULTS AND DISCUSSION

3.1.NMR Spectroscopic analysis

^1H, ^{13}C and ^{19}F and ^{31}P-NMR spectra are used for evaluation and confirmation of the molecular structure of the synthesized ILs $[C_{10}DABCO][Br]$, $[C_{10}DABCO][N(SO_2CF_3)_2]$ and $[C_{10}DABCO][PF_6]$. NMR spectra were analyzed in $CDCl_3$ over the scan range 0 to 10 δ ppm for ^1H NMR (a), from 0 to 100 δ ppm for ^{13}C NMR (b), and in DMSO-d_6 from -120 to -170 δ ppm for ^{31}P NMR (c) and from -100 to -40 δ ppm for ^{19}F NMR of $[C_{10}DABCO][PF_6]$ (d) and from -130 to -30 δ ppm for ^{19}F NMR of $[C_{10}DABCO][N(SO_2CF_3)_2]$ (e). As shown in **Figure 1 (a)** ^1H-NMR analysis of $[C_{10}DABCO][Br]$ shows a triplet between δ= 0.86-0.89 ppm, which is ascribed to the terminal methyl group **(H_1)**, while the two intense signals between δ=1.26-1.34 and 1.60- 1.70 ppm are assigned to methylene protons in the decyl chain **($H_{2\text{-}10}$)**.The latter signals indicated the successful reaction of alkylation in $[C_{10}DABCO][Br]$ that is in accordance with our previous reports [7, 17, 19]. In contrast, the

characteristic peaks for DABCO hydrogens **(H_{11})** appeared at δ=3.16-3.22 ppm; another characteristic peak is observed around δ= 3.29-3.32 ppm and is ascribed to the DABCO deshielded protons **(H_{12})**, consistently with our recent works [7, 17,19]. In the ^{13}C-NMR spectrum of [C_{10}DABCO][Br] (**Figure S1 (b)**), the signals between 14.10 and 31.80 ppm were attributed to the carbons of the decyl chain, the signal found at 65.07 ppm is ascribed to carbon situated near to the DABCO cycle. The spectra in **Figure S1 (c and d)** were recorded for the [C_{10}DABCO][PF_6] in DMSO-d_6. The six fluorines are all equivalent in the [PF_6^-] anion and so the ^{31}P NMR spectrum consists of a septet. The separation between any adjacent pair of peaks is the P-F coupling constant, in this case 711 Hz. Since all six fluorine nuclei are equivalent they couple to just the phosphorus nucleus to give a doublet, again separated by 711 Hz which confirms the anionic exchange of hexafluorophosphate. In [C_{10}DABCO][$N(SO_2CF_3)_2$], the appearance of two new signals in the ^{13}C-NMR spectrum (**Figure S1 (e))** as a doublet at δ = 124.54/122.75 ppm is due to the carbon atoms from the CF_3 groups of the anion.The anionic exchange reaction in [C_{10}DABCO][$N(SO_2CF_3)_2$] is well confirmed by the appearance of a intense singlet centered around −78.85 ppm (**Figure S1 (f))** attributed to fluorine atoms in anion. For an overview, the spectroscopic data are given below and the ^{13}C-NMR **(b)** of [C_{10}DABCO][Br], ^{19}F,^{31}P-NMR **(c-d)** of [C_{10}DABCO][PF_6], ^{13}C,^{19}F -NMR **(e-f)** of ([$N(SO_2CF_3)_2]^-$) spectra are shown in Figure S1 of the supplementary material, respectively.

[C_{10}DABCO][Br]: **^{1}H-NMR**, ($CDCl_3$) δ_H(ppm) =0.86-0.89 (t,3H), 1.26–1.34 (m, 14H), 1.60 (m, 2H),1.70 (m, 2H),3.16-3.22 (t, 6H),3.29-3.32 (t, 6H),**^{13}C-NMR**-[C_{10}DABCO][Br], ($CDCl_3$) δ_C(ppm) = 14.10, 21.67, 22.57, 26.18, 28.72, 29.06, 29.27, 31.80, 45.16, 52.56, 58.50, 65.07.

[C_{10}DABCO][PF_6]**: ^{19}F-NMR** (DMSO-d_6) two signals at:-69.19, -71.08 (δ ppm: -70.13, doublet, J_{FP}=712Hz). **^{31}P-NMR** (DMSO-d_6) seven signals at: -131.03, -135.45, -139.84, -144.24, -148.62, -153.11, 157.35 (δ ppm:-144.24, septuplet, J_{PF}=710Hz).
[C_{10}DABCO][$N(SO_2CF_3)_2$]: **^{13}C-NMR**- anion: 124.54, 122.75, **^{19}F–NMR** (DMSO-d_6) δ_F ppm= −78.85 (s, [$N(SO_2CF_3)_2]^-$).

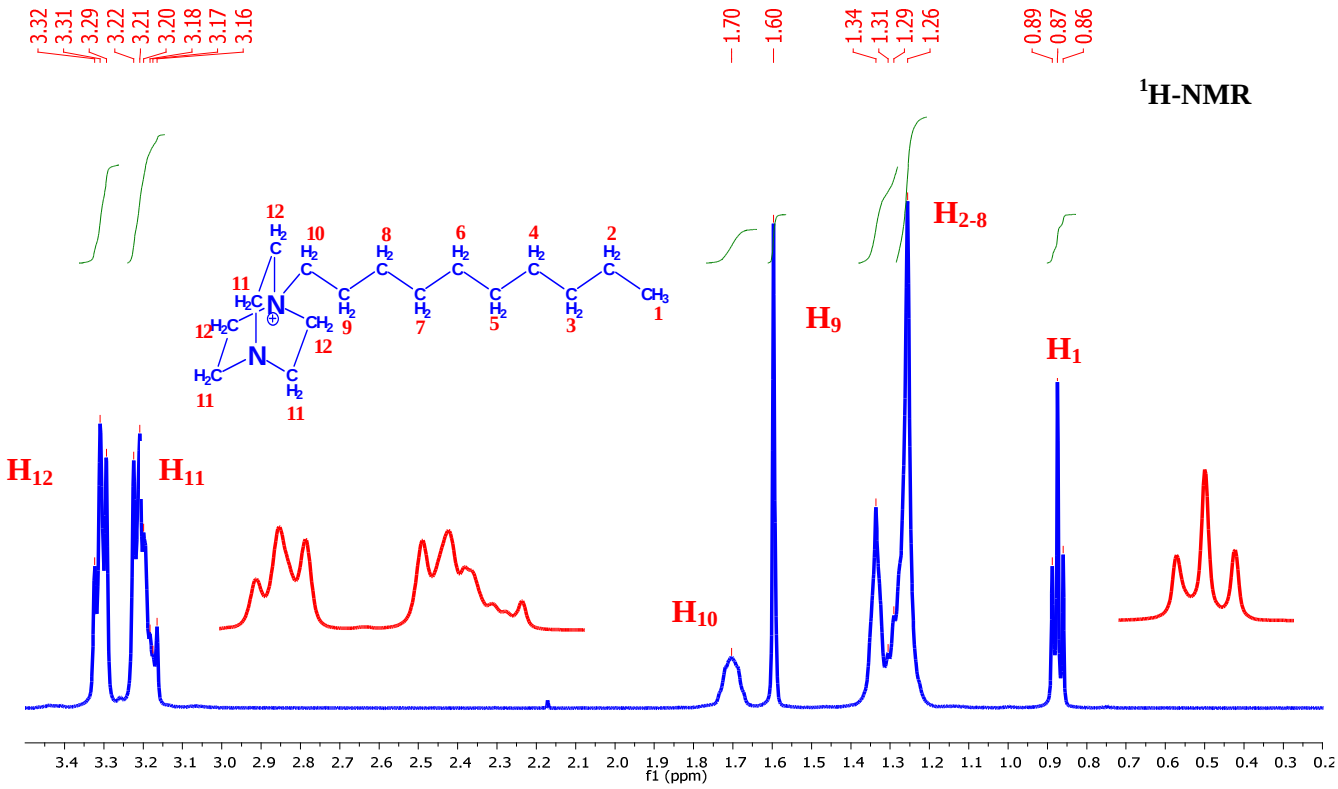

Figure 1. **(a)** Hydrogen atom labeling and ^{1}H-NMR spectrum of the DABCO cation.

3.2.Electrostatic potential (ESP) maps

The electrostatic potential (ESP) maps area useful method to determine the locations with high electron density in anions or low electron density in cations of ILs. It can be used to predict the reaction center of anions with cation in the ILs. The electrostatic potential (ESP) maps obtained for $[C10DABCO]^{+}$ cation and $[Br]^{-}$, $[PF_6]^{-}$, $[N(SO_2CF_3)_2]^{-}$**(s)** and $[N(SO_2CF_3)_2]^{-}$**(as)** anions at M06-2X/AUG–cc–pVDZ level of theory are shown in **Figure.2.** It should be noted that $[N(SO_2CF_3)_2]^{-}$ anion has two configurations, symmetric and asymmetric, which are shown in this paper with the $[N(SO_2CF_3)_2]^{-}$**(s)** and $[N(SO_2CF_3)_2]^{-}$**(as)** symbols, respectively).

Figure.2 shows that the highest negative electron density region is located around the Br atom, F atoms of $[PF_6]^{-}$ anion and O atoms of $[N(SO_2CF_3)_2]^{-}$**(s)** and $[N(SO_2CF_3)_2]^{-}$**(as)** anions while the positive electron density region is mainly located on H4, H18 and H22 atoms of the DABCO ring and alkyl group.

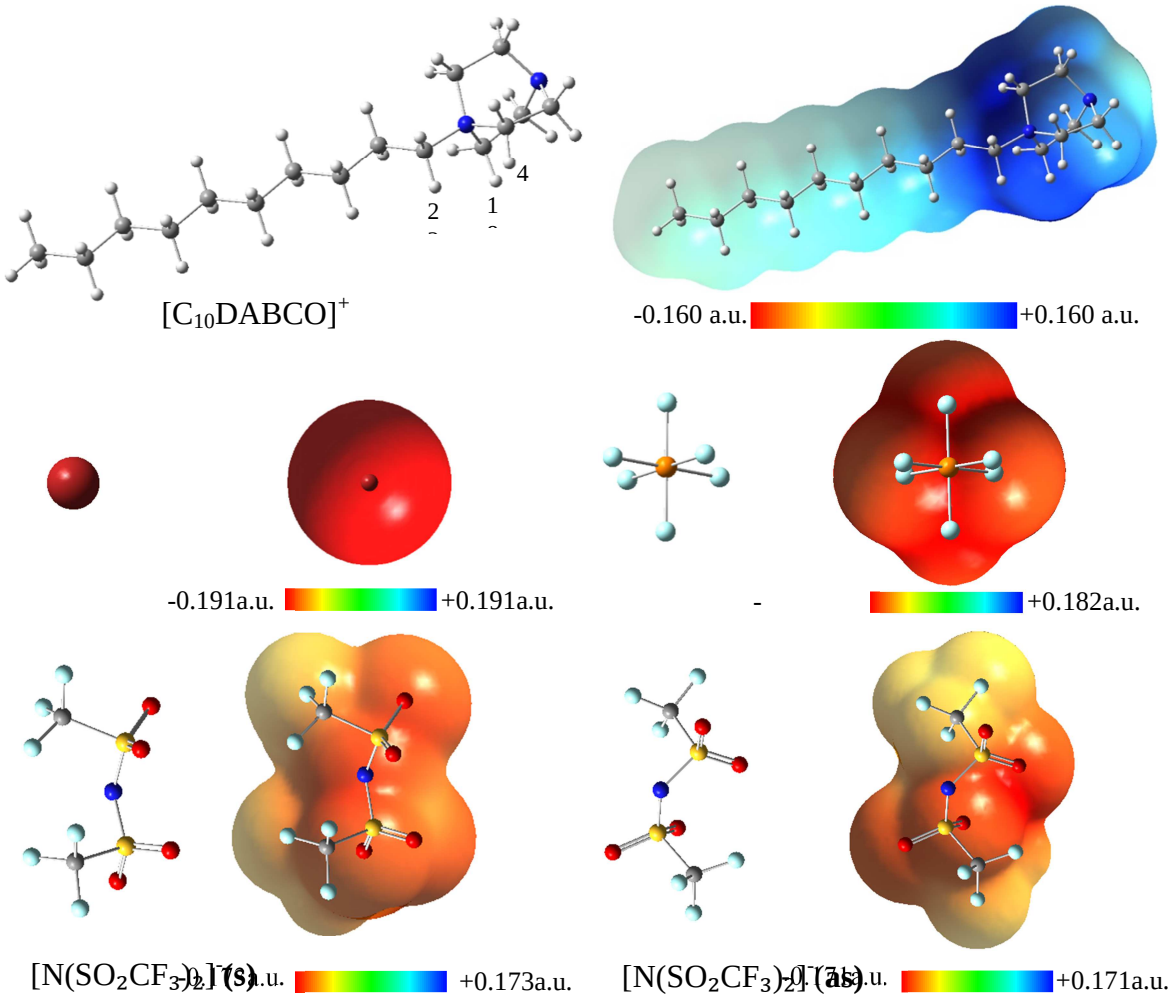

Figure.2. Electrostatic potential (ESP) maps for the cation $[C10DABCO]^+$ and anions $[Br]^-$, $[PF_6]^-$, $[N(SO_2CF_3)_2]^-$**(s)** and $[N(SO_2CF_3)_2]^-$**(as)**at M06-2X-GD3/AUG–cc–pVDZ level of theory.

The large blue region on the DABCO ring indicates that the H4 and H18 atoms of DABCO ring and H22 atom of alkyl group would be the main reactive center in the cation in terms of positive charge density and orientation to form hydrogen bonds with the anions. According to the electrostatic potential maps of the cation and anions, there are a significant number of possible interaction sites around the cation that anions can be interacted with it. After analyzing all the possible conformations of all designed ILs, the configurations reported in **Figure 3** are the most stable for the three ILs.

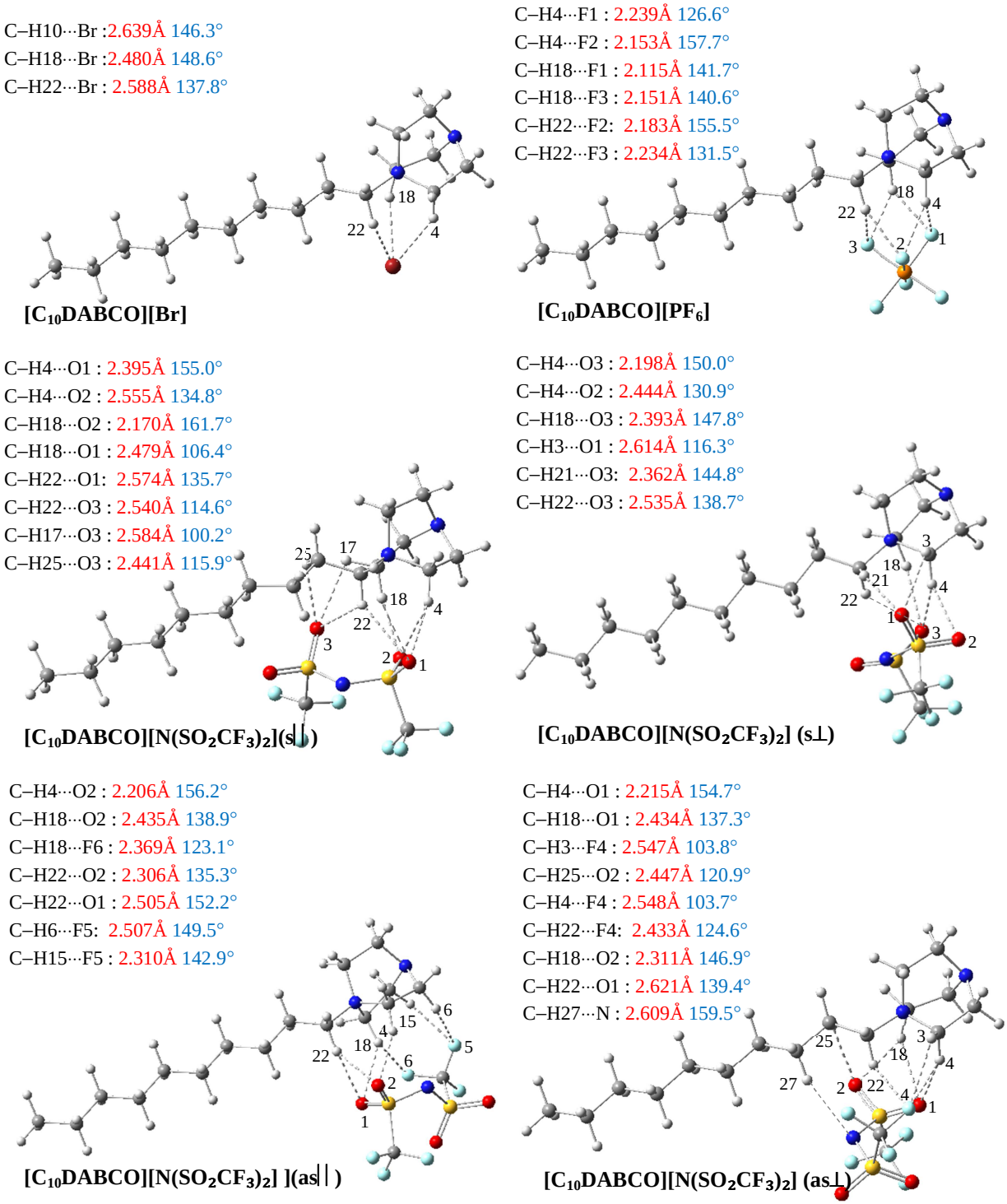

Figure. 3. The optimized structures at M06-2X-GD3/AUG–cc–pVDZ level of theory for [C_{10}DABCO][Br], [C_{10}DABCO][PF_6], [C_{10}DABCO][$N(SO_2CF_3)_2$] **(s|),** [C_{10}DABCO][$N(SO_2CF_3)_2$] **(s⊥),** [C_{10}DABCO][$N(SO_2CF_3)_2$] **(as|)** and[C_{10}DABCO][$N(SO_2CF_3)_2$] **(as⊥)** ILs in gas phase.

This figure shows that spherical $[Br]^-$ and $[PF_6]^-$anions locate above the DABCO ring, near to the alkyl chain in [C_{10}DABCO][Br] and [C_{10}DABCO][PF_6] ILs, while $[N(SO_2CF_3)_2]^-$**(s)** and

$[N(SO_2CF_3)_2]^-$**(as)** anions can be located above the DABCO ring, in a configuration parallel or perpendicular to the alkyl chain in the $[C_{10}DABCO][N(SO_2CF_3)_2]$ **(s∥),** $[C_{10}DABCO][N(SO_2CF_3)_2]$ **(s⊥),** $[C_{10}DABCO][N(SO_2CF_3)_2]$ **(as∥)** and $[C_{10}DABCO][N(SO_2CF_3)_2]$ **(as⊥)** (**∥**) and **(⊥)** refers to the configurations in those the $[N(SO_2CF_3)_2]^-$anion is approached in line with or perpendicular to the cation C10 alkyl chain, respectively).

3.3. Structural parameters

As shown in **Figure. 3**, the interactions between the anion and cation of the studied ILs could be characterized by intermolecular hydrogen bonds of C–H···Br, C–H···F and C–H···O types, that formed mainly between the electronegative Br, F and O atoms of the $[Br]^-$, $[PF_6]^-$, $[N(SO_2CF_3)_2]^-$(s) and $[N(SO_2CF_3)_2]^-$(as) anions and the C–H bonds of the $[C_{10}DABCO]^+$ cation. The H bond lengths and their corresponding angles are shown by dashed lines in **Figure.3**. It should be noted that the IL having $[N(SO_2CF_3)_2]^-$**(s)** and $[N(SO_2CF_3)_2]^-$**(as)** anions adopts the four configurations $[C_{10}DABCO][N(SO_2CF_3)_2]$ **(s∥),** $[C_{10}DABCO][N(SO_2CF_3)_2]$ **(s⊥),** $[C_{10}DABCO][N(SO_2CF_3)_2]$ **(as∥)** and$[C_{10}DABCO][N(SO_2CF_3)_2]$ **(as⊥)**, and the $[C_{10}DABCO][N(SO_2CF_3)_2]$ **(s∥)** structure is more stable than the others. The latter configuration is in good agreement with that reported by Haddad et al. **[**19**]** for DABCO-based ionic liquids containing $[N(SO_2CF_3)_2]^-$ anion.

Generally, a structural measure of existence of H-bonding interaction in ILs is the fact that the distance between the H atom on the donor group of cation and the acceptor atom of anion are lower than the sum of their van der Waals radii. Accordingly, there are three and six hydrogen bonds of C–H···Br and C–H···F type in the $[C_{10}DABCO][Br]$ and$[C_{10}DABCO][PF_6]$ ILs, as shown by dashed lines in **Figure. 3.** While in the ionic liquid containing $[N(SO_2CF_3)_2]^-$ anion, there are 8, 6, 7 and 9 hydrogen bonds, respectively, that are formed between the O or F atoms and C–H bonds of the DABCO ring and alkyl group of cation. The values of hydrogen bond distances and angles between anions and cations in the studied ionic liquids are listed in **Figure.3.** In addition to H-bond distance, the linearity of H-bond angles can be considered as a measure of H bond strength. The structural parameters show that the hydrogen bonding distance (angle) of bond C–H18···Br in $[C_{10}DABCO][Br]$, bond C–H18···F1 in $[C_{10}DABCO][PF_6]$, bond C–H18···O2 in $[C_{10}DABCO][N(SO_2CF_3)_2]$ **(s∥)**, bond C–H18···O3 in $[C_{10}DABCO][N(SO_2CF_3)_2]$ **(s⊥)**, bond C–H18···O1 in $[C_{10}DABCO][N(SO_2CF_3)_2]$ **(as∥)** and bond C–H18···O2 in $[C_{10}DABCO][N(SO_2CF_3)_2]$ **(as⊥)** are 2.480 (148.6), 2.115 (141.7), 2.170 (161.7), 2.393 (147.8), 2.435 (138.9) and 2.311

(146.9) Å (°), respectively. It is expected that the strength of these hydrogen bonds in each of the studied ionic liquids can be larger than that of the other hydrogen bonds in each IL. Also, the average of the hydrogen bond distances (angles) in $[C_{10}DABCO][Br]$, $[C_{10}DABCO][PF_6]$, $[C_{10}DABCO][N(SO_2CF_3)_2]$ **(s||),** $[C_{10}DABCO][N(SO_2CF_3)_2]$ **(s⊥),** $[C_{10}DABCO][N(SO_2CF_3)_2]$ **(as||)** and $[C_{10}DABCO][N(SO_2CF_3)_2]$ **(as⊥)** ILs are 2.569 (144.3), 2.179 (142.3), 2.468 (128.0), 2.179 (142.3), 2.468 (128.0) and 2.424 (138.1) Å (°), respectively. The results show that the position of anions relative to the cation in $[C_{10}DABCO][PF_6]$, $[C_{10}DABCO][N(SO_2CF_3)_2]$ **(s||),** $[C_{10}DABCO][N(SO_2CF_3)_2]$ **(s⊥),** $[C_{10}DABCO][N(SO_2CF_3)_2]$ **(as||)** and $[C_{10}DABCO][N(SO_2CF_3)_2]$ **(as⊥)** ILs is not suitable for a strong H-bonding interaction to occur.

3.4. Interaction energies

The interaction energies (ΔE) in the investigated ILs are calculated using equation **(1)**at M06-2X/AUG–cc–pVDZ level of theory in gas phase.

ΔE_{elec} (IL) = E_{elec}(IL) - (E_{elec}(cation)) – E_{elec}(anion)) **(1)**

The values of interaction energies of the ILs were corrected by basis set superposition errors (BSSE) and zero-point vibrational energies (ZPVE). In addition, since the interactions between the $[C_{10}DABCO]^+$ cation and $[Br]^-$, $[PF_6]^-$, $[N(SO_2CF_3)_2]^-$**(s)** and $[N(SO_2CF_3)_2]^-$**(as)** anions in the studied ILs are influenced by van derWaals interactions, the interaction energies were corrected by the inclusion of empirical dispersion at the same level of theory. The calculated interaction energy (ΔE_c), Gibbs free energy (ΔG_c) and enthalpy (ΔH_c) of $[C_{10}DABCO][Br]$, $[C_{10}DABCO][PF_6]$, $[C_{10}DABCO][N(SO_2CF_3)_2]$ **(s||),** $[C_{10}DABCO][N(SO_2CF_3)_2]$ **(s⊥),** $[C_{10}DABCO][N(SO_2CF_3)_2]$ **(as||)** and $[C_{10}DABCO][N(SO_2CF_3)_2]$ **(as⊥)** ILs are calculated using equation **(2)** in the gas phase and are summarized in **Table 1**.

ΔX_c (IL) = ΔX_{elec}(IL) + BSSE + ΔZPVE + ΔE_{disp} X: E, G and H **(2)**

Table 1

Interaction thermodynamic parameters (ΔE, ΔH and ΔG (in kcal mol^{-1}) calculated for $[C_{10}DABCO][Br]$, $[C_{10}DABCO][PF_6]$, $[C_{10}DABCO][N(SO_2CF_3)_2]$ **(s||),** $[C_{10}DABCO][N(SO_2CF_3)_2]$ **(s⊥),** $[C_{10}DABCO][N(SO_2CF_3)_2]$ **(as||)** and$[C_{10}DABCO][N(SO_2CF_3)_2]$ **(as⊥)** ILs at M06-2X-GD3/AUG–cc–pVDZ level of theory. All quantities are given with a±0.01 kcal mol^{-1}uncertainty.

ILs	ΔE	ΔZPVE	BSSE	$\%\Delta E_{disp}$	ΔE_c	ΔH_c	ΔG_c
$[C_{10}DABCO][Br]$	-89.93	0.18	0.65	1.92	-90.86	-90.81	-83.62
$[C_{10}DABCO][PF_6]$	-81.98	1.14	2.40	2.86	-80.85	-79.17	-68.01
$[C_{10}DABCO][N(SO_2CF_3)_2]$ **(s||)**	-83.86	1.07	3.88	4.18	-82.57	-81.09	-68.14

$[C_{10}DABCO][N(SO_2CF_3)_2]$ **(s⊥)**	-80.71	0.97	3.32	4.04	-79.82	-78.23	-66.71
$[C_{10}DABCO][N(SO_2CF_3)_2]$ **(as||)**	-74.77	0.84	3.00	4.30	-74.29	-72.94	-61.01
$[C_{10}DABCO][N(SO_2CF_3)_2]$ **(as⊥)**	-78.04	1.29	3.56	4.52	-76.87	-75.17	-62.09

As can be seen in **Table 1**, the corrected interaction energy (ΔEc) values of $[C_{10}DABCO][Br]$, $[C_{10}DABCO][PF_6]$, $[C_{10}DABCO][N(SO_2CF_3)_2]$ **(s||),** $[C_{10}DABCO][N(SO_2CF_3)_2]$ **(s⊥),** $[C_{10}DABCO][N(SO_2CF_3)_2]$ **(as||)** and $[C_{10}DABCO][N(SO_2CF_3)_2]$ **(as⊥)** ILs are -90.86, -80.85, -82.57, -79.82, -74.29 and -76.87 kcal mol^{-1}. The percentage of increase in interaction energy upon dispersion correction for the studied ILs is 1.92, 2.86, 4.18, 4.04, 4.30 and 4.50, respectively. The contribution of dispersion energies obtained by using M06-2X-D3 functional for $[C_{10}DABCO][N(SO_2CF_3)_2]$ **(s||),** $[C_{10}DABCO][N(SO_2CF_3)_2]$ **(s⊥),** $[C_{10}DABCO][N(SO_2CF_3)_2]$ **(as||)** and $[C_{10}DABCO][N(SO_2CF_3)_2]$ **(as⊥)** ILs are higher than for $[C_{10}DABCO][Br]$ and $[C_{10}DABCO][PF_6]$ ILs. The corrected interaction energy values for different configurations of ionic liquids containing $[N(SO_2CF_3)_2]^-$ anions show that $[C_{10}DABCO][N(SO_2CF_3)_2]$ **(s||)** configuration for symmetrical type anion of $[N(SO_2CF_3)_2]^-$**(s)** and $[C_{10}DABCO][N(SO_2CF_3)_2]$ **(as⊥)** configuration for asymmetric type anion of $[N(SO_2CF_3)_2]^-$ **(as)** are more stable than the other mentioned configurations. In general, the most stable configuration among the fourones of this series of ionic liquids is the $[C_{10}DABCO][N(SO_2CF_3)_2]$ **(s||)** configuration. Therefore, in the continuation of the theoretical studies, we will only examine the most stable configuration of the studied ionic liquids, i.e. $[C_{10}DABCO][Br]$, $[C_{10}DABCO][PF_6]$ and $[C_{10}DABCO][N(SO_2CF_3)_2]$ **(s||)** ILs. Based on the calculated ΔE_c, the predicted stability order for the ILs formed from interaction between $[C_{10}DABCO]^+$ cation and $[Br]^-$, [PF6]- and $[N(SO_2CF_3)_2]^-$ anions is $[C_{10}DABCO][Br]$ (-90.86 kcal mol^{-1}) > $[C_{10}DABCO][N(SO_2CF_3)_2]$ **(s||)** (-82.57 kcal mol^{-1}) >$[C_{10}DABCO][PF_6]$ (-80.85 kcal mol^{-1}). It is clear that the most and least stable structures correspond to ILs formed from the interaction of $[C_{10}DABCO]^+$ cation with $[Br]^-$ and $[PF_6]^-$ anions, respectively. According to the results given in **Table 1**, the ILs composed of the anions with stronger basicity show the stronger interaction with the cation compared with weaker ones.

3.5. Non-covalent interaction (NCI) and atoms in molecule (AIM) analysis

The Non-covalent interaction (NCI) technique is used to detect non-covalent interactions such as van der Waals (vdW) interactions, hydrogen bonds and steric repulsion in the molecular systems. The reduced density gradient diagram (RDG) and the NCI index are based on the electron density and its derivatives, and are reported in blue, red, and green color dependenly on $\lambda_2(r) \times \rho(r)$ values to indicate hydrogen bonds, strong repulsion interactions and vdW interaction, respectively. **Figure. 4** shows the $\lambda_2(r) \times \rho(r)$ sign isosurfaces and the RDG versus $\lambda_2(r) \times \rho(r)$ sign plots of $[C_{10}DABCO][Br]$, $[C_{10}DABCO][PF_6]$ and $[C_{10}DABCO][N(SO_2CF_3)_2]$ **(s||)** ILs to reveal noncovalent interactions. As can be seen, these figures confirm the existence of non-covalent interactions such as van der Waals (vdW) interactions and weak hydrogen bond interactions between the cation and the anions and also and steric repulsion in rings of the studied ILs.

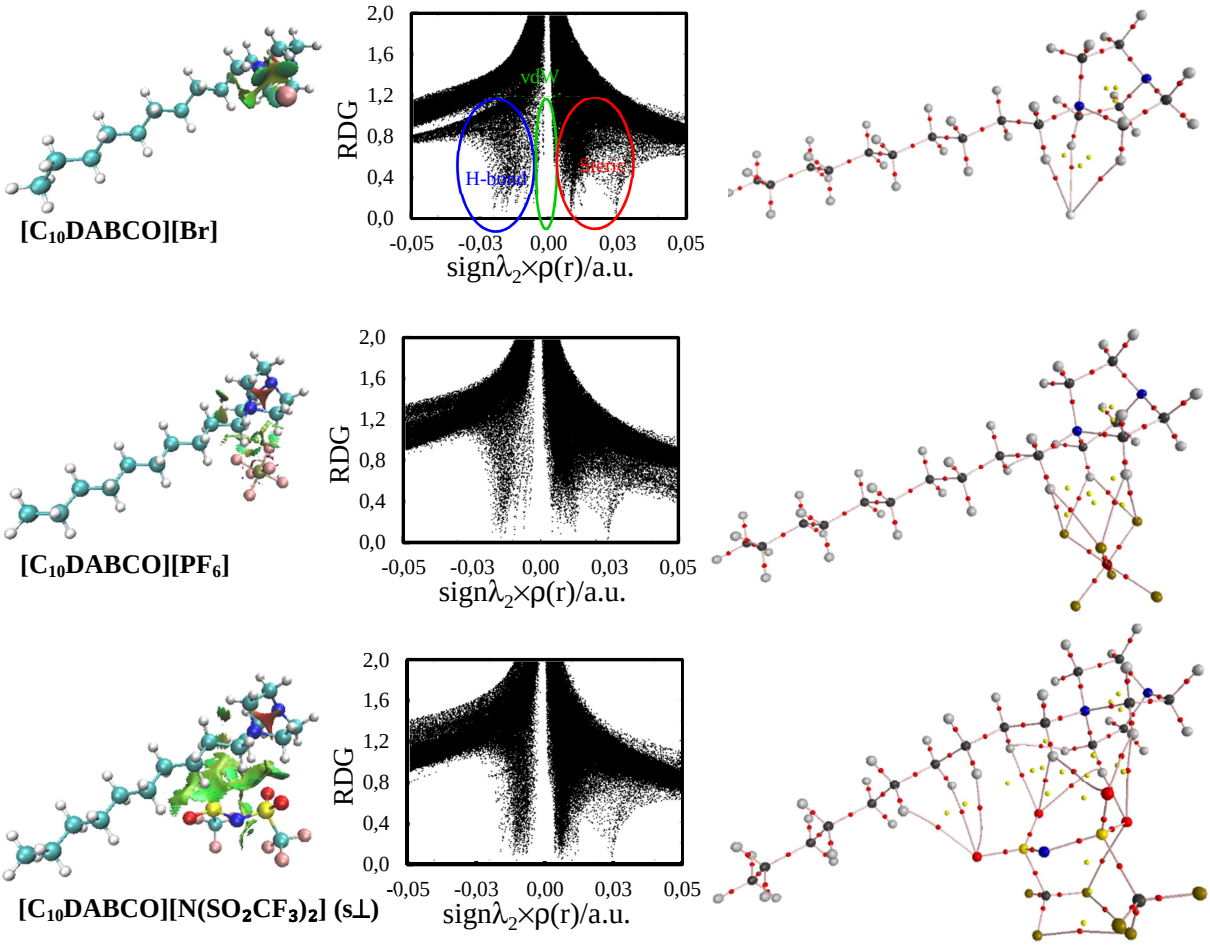

Figure. 4. RDG isosurfaces (s = 0.5 a.u.), plots of RDG isosurfaces versus sign $(\lambda_2) \times \rho(r)$ and molecular graphs from topological analysis of $[C_{10}DABCO][Br]$, $[C_{10}DABCO][PF_6]$ and $[C_{10}DABCO][N(SO_2CF_3)_2]$ **(s||)** ILs.

Topological parameters derived from the quantum theory of atoms in molecules (QTAIM) are useful quantities to determine the nature of intermolecular and intramolecular hydrogen bonds interactions in the ILs. Topological data such as electronic density, ρ(r), its Laplacian, $\nabla^2\rho(r)$, and electronic energy density, H(r), electronic kinetic energy density, G(r), and electronic potential energy density, V(r) at the hydrogen bond critical points (HBCPs) and the molecular graphs including the covalent and non-covalent bond critical points (BCPs), hydrogen bond critical points (HBCPs), ring critical points (RCPs) and bond paths for [C_{10}DABCO][Br], [C_{10}DABCO][PF_6] and [C_{10}DABCO][$N(SO_2CF_3)_2$] **(s|)** ILs are shown in **Table 2** and **Figure.4**.

Table 2
Topological properties of the electron density (a.u.) calculated for most stable [C_{10}DABCO][Br], [C_{10}DABCO][PF_6] and [C_{10}DABCO][$N(SO_2CF_3)_2$] **(s|)** ILs.

	ρ(r)	Lρ(r)	$\nabla^2\rho(r)$	K(r)	V(r)	H(r)
[C_{10}DABCO][Br]						
C–H4···Br	0.0153	-0.0090	0.0360	0.0089	-0.0087	0.0001
C–H18···Br	0.0199	-0.0120	0.0480	0.0119	-0.0118	0.0001
C–H22···Br	0.0169	-0.0103	0.0413	0.0102	-0.0100	0.0002
[C_{10}DABCO][PF_6]						
C–H4···F1	0.0143	-0.0131	0.0525	0.0127	-0.0122	0.0004
C–H4···F2	0.0155	-0.0135	0.0538	0.0133	-0.0130	0.0002
C–H18···F1	0.0175	-0.0155	0.0619	0.0153	-0.0152	0.0001
C–H18···F3	0.0162	-0.0144	0.0577	0.0142	-0.0139	0.0002
C–H22···F2	0.0147	-0.0129	0.0515	0.0126	-0.0122	0.0003
C–H22···F3	0.0142	-0.0127	0.0509	0.0124	-0.0120	0.0003
[C_{10}DABCO][$N(SO_2CF_3)_2$] **s(| |)**						
C–H4···O1	0.0114	-0.0085	0.0341	0.0084	-0.0082	0.0001
C–H4···O2	0.0092	-0.0074	0.0295	0.0069	-0.0064	0.0005
C–H18···O2	0.0161	-0.0133	0.0530	0.0125	-0.0118	0.0007
C–H22···O1	0.0098	-0.0082	0.0327	0.0073	-0.0065	0.0009
C–H17···O3	0.0107	-0.0103	0.0414	0.0089	-0.0075	0.0014
C–H22···O3	0.0104	-0.0087	0.0347	0.0081	-0.0075	0.0006
C–H25···O3	0.0112	-0.0101	0.0404	0.0091	-0.0081	0.0010
C–H27···O4	0.0076	-0.0064	0.0257	0.0056	-0.0048	0.0008
C–H30···O4	0.0067	-0.0061	0.0243	0.0052	-0.0043	0.0009
C–H33···O4	0.0063	-0.0058	0.0234	0.0050	-0.0041	0.0009

The sum of electron density at all hydrogen bond critical points ($\Sigma\rho(r)_{C-H\cdots Br\text{ or }F\text{ or }O}$) can be considered as a measure of the strength of hydrogen bond interactions. The sum of electron densities at all hydrogen bond critical points, ($\Sigma\rho(r)_{C-H\cdots Br\text{ or }F\text{ or }O}$), of [$C_{10}$DABCO][Br],

[C_{10}DABCO][PF_6] and [C_{10}DABCO][$N(SO_2CF_3)_2$] **(s|)** ILs is 0.0173, 0.0154 and 0.0099 a.u., respectively. This value is higher in[C_{10}DABCO][Br] higher than in [C_{10}DABCO][PF_6] and [C_{10}DABCO][$N(SO_2CF_3)_2$] **(s|),** which is in agreement with the interaction energy trends obtained for those ionic liquids.

As discussed above in the geometrical structure section, hydrogen bond C–H18···Br in [C_{10}DABCO][Br] IL, hydrogen bond C–H18···F1 in [C_{10}DABCO][PF_6] IL and hydrogen bond C–H18···O2 in [C_{10}DABCO][$N(SO_2CF_3)_2$] IL have the smallest distance and the largest hydrogen bond angle, in other words, they are closer to a standard hydrogen bond in terms of angle and distance. The results of AIM data in **Table 2** also show that the electron density of the mentioned hydrogen bonds is also higher than that of the other hydrogen bonds in each of the ionic liquids. The hydrogen bond energies ($E_{H...Y}$) are also calculated using equation **(3)** [36]:

$E_{H...Y} = (1/2)V(r)$ **(3)**

On the other hand, half of the electronic potential energy density value of a hydrogen bond indicates the strength of the hydrogen bond in the bond. The values of V(r) in hydrogen bonds C–H18···Br, C–H18···F1 and C–H18···O2 are higher than other hydrogen bonds in any of the studied ionic liquids. The sign and the magnitude of Laplacian of the electron density ($\nabla^2\rho$®) and electronic density energy®(r)) at the HBCPs can be used to investigate the nature of the hydrogen bond interactions between the studied anions and cation in [C_{10}DABCO][Br], [C_{10}DABCO][PF_6] and [C_{10}DABCO][$N(SO_2CF_3)_2$] **(s|)** ILs. Data in **Table 2** show that the sign of both $\nabla^2\rho(r)$ and H(r) in all hydrogen bond critical points in [C_{10}DABCO][Br], [C_{10}DABCO][PF_6] and [C_{10}DABCO][$N(SO_2CF_3)_2$] **(s|)** ILs are positive, indicating that the nature of these hydrogen bonds is electrostatic.

3.6. Natural bond orbital (NBO) and frontier molecular orbital (FMO) analysis

The natural bond orbital (NBO) calculations is a useful technique for evaluation of the atomic charge distribution in the ILs. The results of NBO including natural charge of atoms and charge transfer (CT) values are summarized in **Table 3**. The NBO charge analysis reveals that a charge transfer (CT) occurs from the anions to the $[C_{10}DABCO]^+$ cation upon the formation of the ion pair.

Table 3
NBO data, HOMO and LUMO energy and HOMO–LUMO energy gap calculated for [C_{10}DABCO][Br], [C_{10}DABCO][PF_6] and [C_{10}DABCO][$N(SO_2CF_3)_2$] **(s|)** ILs, isolated cation and anions at M06–2X-GD3/AUG–cc–pVDZ level of theory in gas phase.

$[Br]^-$	$[PF_6]^-$	$[N(SO_2CF_3)_2]$	$^a[D]^+$	[D][Br]	[D][PF_6	[D][$N(SO_2CF_3)_2$

			-			]	] s(|)
q_{H4}				0.2599	0.3047	0.3018	0.2868
q_{H17}				0.2596	0.2327	0.2426	0.2596
q_{H18}				0.2527	0.3118	0.3015	0.2968
q_{H22}				0.2534	0.3039	0.2979	0.2501
q_{H25}				0.2366	0.2583	0.2481	0.2531
CT					0.1081	0.0500	0.0816
q_{Br}	-1.0000				-0.8919		
q_{F1}		-0.6281				-0.6384	
q_{F2}		-0.6281				-0.6274	
q_{F3}		-0.6281				-0.6346	
q_{O3}			-0.9648				-0.9928
q_{O1}			-0.9591				-0.9610
q_{O2}			-0.9501				-0.9781
E_{LUMO}				-3.32	-0.78	-0.91	-0.87
E_{HOMO}	-2.13	-7.71	-5.96		-6.42	-8.88	-8.94
E_{gap}					5.64	7.97	8.08

[a]: D=C_{10}DABCO

The hydrogen bond interactions between the cation and anions in [C_{10}DABCO][Br], [C_{10}DABCO][PF_6] and [C_{10}DABCO][$N(SO_2CF_3)_2$] **(s|)** ILs lead to an increase of the positive charge of atoms of H4, H18 and H22 as well as, decrease the negative charge of Br, F and O atoms compared to those charges on isolated cation and anions. The transferred charge values from anions to cation in [C_{10}DABCO][Br], [C_{10}DABCO][PF_6] and [C_{10}DABCO][$N(SO_2CF_3)_2$] **(s|)** ILs are about 0.1081, 0.0500 and 0.0816 a.u., respectively. As can be observed, the increase in the interaction energies is accompanied by an increase in CT value of [C_{10}DABCO][Br], [C_{10}DABCO][PF_6] and [C_{10}DABCO][$N(SO_2CF_3)_2$] **(s|)** ILs. The CT decreases on going from $[Br]^-$ anion to $[PF_6]^-$ one as the interaction energy decreases. The charge transfer is an important factor which could be used when stability of the ILs is under consideration. It is well known that the charge transfer value has a direct relation to stability and interaction energy of the ILs in a way that the increase of it leads to form more stable ionic liquid configuration. Frontier molecular orbitals (FMOs) play a key role in determination of stability, reactivity and electric properties of ILs. FMOs diagram in ILs are useful for understanding the intermolecular interactions, especially charge transfer process. In the ILs generally LUMO of cation and HOMO of anion are very important, because, the charge transfer occurrs from the HOMO orbital of anion to the LUMO orbital of cation. Therefore, as the energy difference between HOMO and LUMO orbitals decreases and the charge transfer increases, stronger interactions will be formed. The energy of the HOMO orbital of the anions can be sufficient to determine the easiness of the charge transfer from the anionic part to the cationic part, that is directly related to the strength of the formed

interaction between cation and anion in an ionic liquid. The FMOs energy diagram for $[C_{10}DABCO][Br]$, $[C_{10}DABCO][PF_6]$ and $[C_{10}DABCO][N(SO_2CF_3)_2]$ **(s|)** ILs are depicted in **Figure. 5**. As shown in **Figure. 5**, LUMO of cation is a σ* molecular orbital in nature (E_{LUMO}= -3.32 eV) and HOMO of the anions are localized on Br atom, six P–F bonds and four S=O bonds in $[Br]^-$, $[PF_6]^-$ and $[N(SO_2CF_3)_2]^-$anions, respectively. HOMO energy values for anions are -2.13, -7.71 and -5.96 eV respectively for $[Br]^-$, $[PF_6]^-$ and $[N(SO_2CF_3)_2]^-$ anions. An analysis of the HOMO orbitals of $[C_{10}DABCO][Br]$ IL reveals that they consist of p orbitals of Br atom and σ bond orbital of C–H bonds. In $[C_{10}DABCO][PF_6]$ IL, the HOMO orbitals is composed by σ orbitals of DABCO ring of the cationic part, while the HOMO orbitals in $[C_{10}DABCO][N(SO_2CF_3)_2]$ **(s|)** IL is due to both anion and cation parts. The distribution of LUMO orbitals is different from HOMO ones in the ILs. They are mainly identical and antibonding σ*orbitals. The LUMO orbitals of the studied ILs are mainly distributed on DABCO ring of the cationic part.

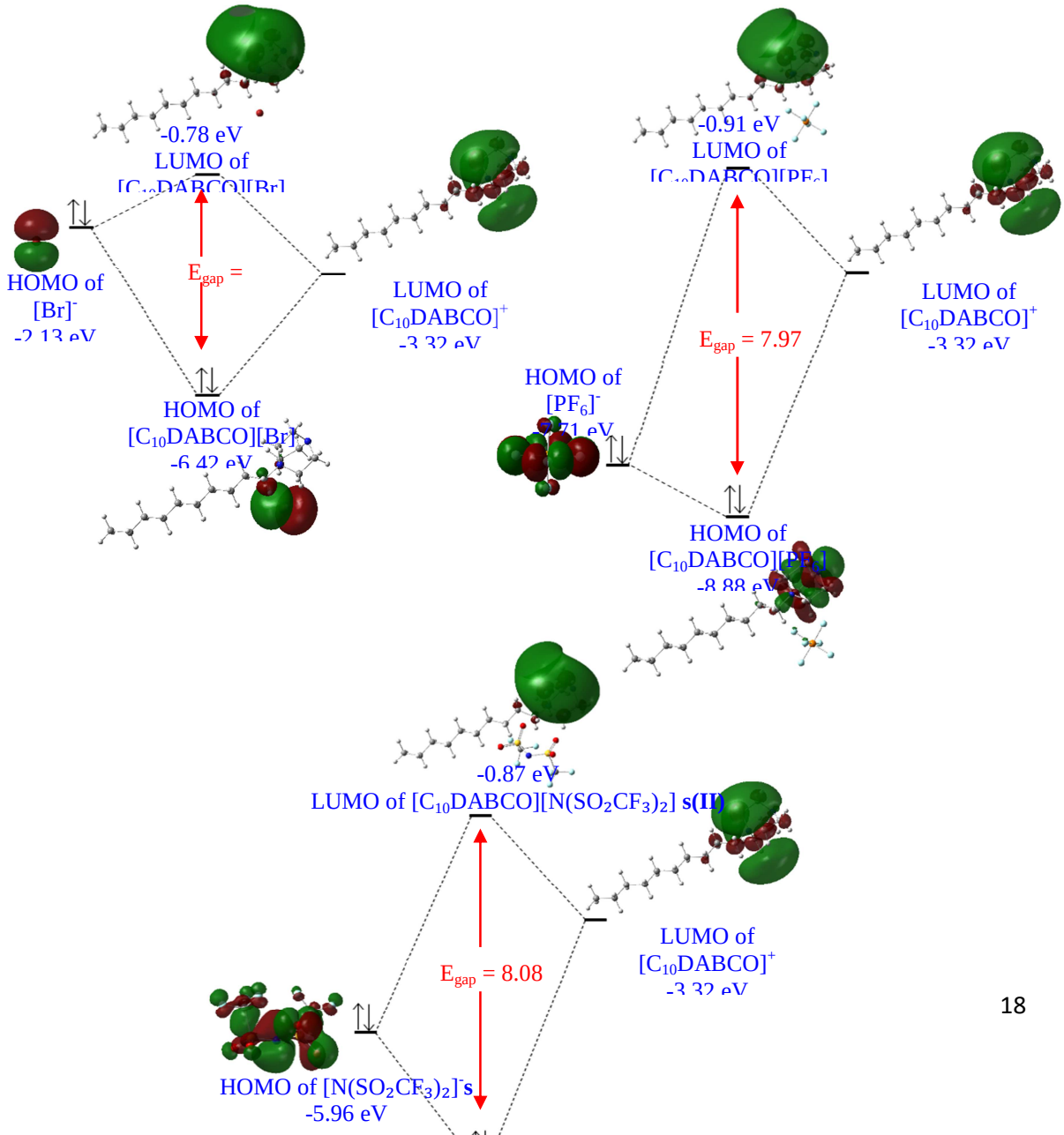

Figure. 5. Frontier molecular orbital (FMO) energy diagrams of $[C_{10}DABCO][Br]$, $[C_{10}DABCO][PF_6]$ and $[C_{10}DABCO][N(SO_2CF_3)_2]$ **(s|)** ILs at M06–2X-GD3/AUG–cc–pVDZ level of theory in gas phase.

Considering the HOMOs location on the anionic part, also LUMOs on the cationic one in the frontier molecular orbital energy diagrams, it is clear that CT occurs from the anions to cation and the anionic part acts as an electron donating part during ionic liquid formation. Also, the HOMO-LUMO energy gap (E_{gap}) defined as the energy difference between HOMO and LUMO, has an important role in chemical reactivity and the structural stability of ILs. The value of HOMO–LUMO energy gap for $[C_{10}DABCO][Br]$, $[C_{10}DABCO][PF_6]$ and $[C_{10}DABCO][N(SO_2CF_3)_2]$ **(s|)** ILs is 5.64, 7.97 and 8.08 eV, respectively. It was clear that the E_{gap} in the studied ILs decreased with $[Br]^-$ anion and increased with $[N(SO_2CF_3)_2]^-$ anion, implying an increase in reactivity of the $[C_{10}DABCO][Br]$ IL and a decrease in reactivity of the $[C_{10}DABCO][N(SO_2CF_3)_2]$ **(s|)** IL.

3.7. Electrochemical window (ECW)

The electrochemical stability of an ionic liquid is determined by the width of the electrochemical window (ECW), the voltage range in which the IL is electrochemically inert. The ECW of ILs depends mostly on the resistance of the anion against oxidation and the resistance of the cation against reduction. Its value can also be predicted by quantum chemical calculations such as DFT by using the HOMO and LUMO energy levels of isolated cation and anions and the potentials of cathodic and anodic limits (V_{CL} and V_{AL})in acetonitrile solvent. ECW values of $[C_{10}DABCO][Br]$, $[C_{10}DABCO][PF_6]$ and $[C_{10}DABCO][N(SO_2CF_3)_2]$ **(s|)** ILs were calculated using CPCM (COSMO-RS) approach at BVP86/TZVP level of theory and were estimated from the following equations:

$$V_{AL} = -E_{HOMO}/e^- = V_{AL}^{CPCM} = \min (V_{AL,C}^{CPCM}, V_{AL,A}^{CPCM}) \quad \textbf{(4)}$$

$V_{CL} = -E_{LUMO}/e^- = V_{CL}^{CPCM} = \max (V_{CL,C}^{CPCM}, V_{CL,A}^{CPCM})$ **(5)**

$ECW = V_{AL} - V_{CL}$ **(6)**

The HOMO and LUMO energy levels of isolated cation and anions, values of ECW and the potentials of the cathodic (V_{CL}) and anodic limits (V_{AL}) of ILs[C_{10}DABCO][Br], [C_{10}DABCO][PF_6] and [C_{10}DABCO][$N(SO_2CF_3)_2$] **(s|)** ILs are listed in **Table 4**. There is a minor change in ECW for the ILs with different anions, although all ILs have wide ECWs 4.79–5.48 V. The cathodic limits of the studied ILs with the same cation follows the sequence of [C_{10}DABCO][$N(SO_2CF_3)_2$] **(s|)** >[C_{10}DABCO][Br] ≈[C_{10}DABCO][PF_6] and comparison of HOMO energy of the anions with HOMO energy of the cation in the ILs shows that anodic stabilities can be characterized by the cation. Thus, the anodic limits of the ILs are similar and about 5.55 V and are in good agreement with those of reported by Ong et al. [37].

Table 4
The LUMO and HOMO energies of free cation and anions, the potentials of the cathodic (V_{CL}) and anodic limits (V_{AL}) and ECW of ILs using CPCM (COSMO-RS)method at BVP86/TZVP level of theory in acetonitrile solvent.

	$[C_{10}DABCO]^+$	$[Br]^-$	$[PF_6]^-$	$[N(SO_2CF_3)_2]^-$s
LUMO	-0.07	6.39	0.26	-0.77
HOMO	-5.55	-5.69	-8.43	-7.10
EA	0.07	-6.39	-0.26	0.77
IE	5.55	5.69	8.43	7.10
		$[C_{10}DABCO][Br]$	**$[C_{10}DABCO][PF_6]$**	**$[C_{10}DABCO][N(SO_2CF_3)_2]$ s(|)**
V_{CL}		0.07	0.07	0.77
V_{AL}		5.55	5.55	5.55
ECW		5.48	5.48	4.79

ECW values of [C_{10}DABCO][Br], [C_{10}DABCO][PF_6] and [C_{10}DABCO][$N(SO_2CF_3)_2$] **(s|)** ILs are 5.48, 5.48 and 4.79 V. Therefore, [C_{10}DABCO][Br] and [C_{10}DABCO][PF_6] ILs have the widest ECW at 5.48 V and [C_{10}DABCO][$N(SO_2CF_3)_2$] **(s|)** IL has the narrowest ECW at 4.79V that it is most likely due to the thermal stability of [C_{10}DABCO][$N(SO_2CF_3)_2$] **(s|)** IL. It is predicted that [C_{10}DABCO][Br] and [C_{10}DABCO][PF_6]ILs with the ECW about 5.48 V have more electrochemical stability than [C_{10}DABCO][$N(SO_2CF_3)_2$] **(s|)** IL for use in electrochemical devices.

3.7. Vibrational spectroscopy analysis:

The experimental FT-IR [600-4000 cm^{-1}] and FT-Raman [45-3500 cm^{-1}] spectra of the three investigated ILs [C_{10}DABCO][Br], [C_{10}DABCO][PF_6] and [C_{10}DABCO][$N(SO_2CF_3)_2$], measured at room temperature are shown in **Figure 6**. The assignment of infrared and Raman vibration frequencies are reported in **Tables S1-S2** of the Supporting Information and the discussion of assignment of the most important vibrations is presented as follows:

3.7.1. Cations vibrations:

The [C_{10}DABCO] cation consists of 50 atoms. The vibrational modes have been assigned according to our three published works [7, 17, 19]. The antisymmetric and symmetric stretching modes of CH_2 and CH_3 groups of cation are observed in the region 3500-2700 cm^{-1}**,** the intense bands observed at 2854/2923 for FT-IR spectra and at 2853/2938 for FT-Raman spectra in [C_{10}DABCO][Br], 2846/2931 for FT-IR spectra and at 2844/2965 for FT-Raman spectra in [C_{10}DABCO][PF_6], 2852/2925 for FT-IR spectra and at 2852/2935 for FT-Raman spectra [C_{10}DABCO][$N(SO_2CF_3)_2$] are assigned to symmetric CH_2 stretching modes, while the strong band located in FT-Raman spectra at 2892 cm^{-1} in [C_{10}DABCO][Br], 2894 cm^{-1} in [C_{10}DABCO][PF_6], 2897 cm^{-1} in [C_{10}DABCO][$N(SO_2CF_3)_2$] can be assigned to symmetric CH_3 stretching mode [7, 19, 38-40].

For the three investigated ILs, the CH_3 deformation modes are observed in the region 1500-1300 cm^{-1}. Also, the strong infrared and Raman bands which are located at1056 cm^{-1}in [C_{10}DABCO][Br], 1058 cm^{-1} in [C_{10}DABCO][PF_6] and at 1055 cm^{-1} in [C_{10}DABCO][$N(SO_2CF_3)_2$] cm^{-1} are assigned to C-C and C-N stretching modes. The CH_2 twisting modes are observed between 900 and 600 cm^{-1} and are in good agreement with our recent values. It has been noted that the vibrational modes are corresponding to the anion together with CH_3 and CH_2 twisting and C-C and C-N stretching and CCN, CCC skeletal modes are observed in the regions of below 1000 cm^{-1} [38, 40-44].

The bands observed at 702, 700 and 703 cm^{-1}in FT-IR spectra are assigned to CH_2 twisting vibrations [42, 44]. The same vibrations in FT-Raman spectrum are at 795, 794, 795 cm^{-1}, respectively.

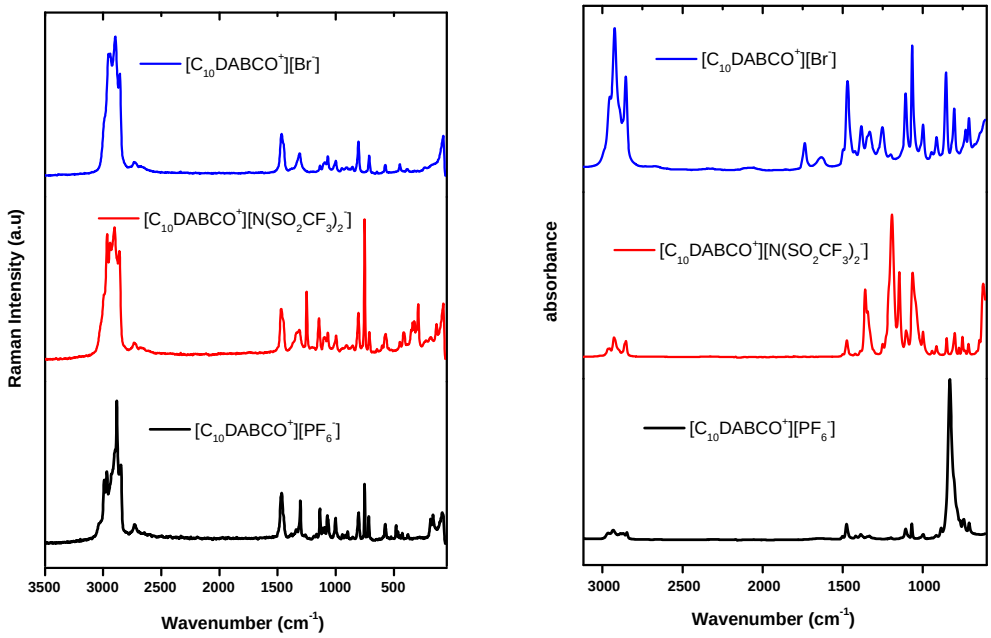

Figure 7. Experimental FT-IR and FT-Raman vibrational spectra of $[C_{10}DABCO][Br]$, $[C_{10}DABCO][PF_6]$ and $[C_{10}DABCO][N(SO_2CF_3)_2]$.

3.7.2. Anions vibrations:

The observed bands of the P–F stretching vibrations in $[C_{10}DABCO][PF_6]$ IL have been found to be very strong in the Raman spectra and these appear in the range 900-700 cm^{-1} and 600-200 cm^{-1} (**Figure 6**).

Also, the antisymmetric P-F stretching modes are observed at 821 $cm^{-1}$for FT-IR spectra and 888 cm^{-1} for Raman spectra while the symmetric stretching mode is assigned to the Raman band at 734 cm^{-1} for FT-IR spectra 470 cm^{-1} for FT-Raman spectra [17-45].

For the $[N(SO_2CF_3)_2]^-$anion, the antisymmetric and symmetric stretching modes of SO_2 and CF_3 groups are located from 1244 to 1028 cm^{-1}[19, 40, 46-47]. In some cases, the antisymmetric SO_2 and CF_3 stretching modes are coupled between them. Moreover, the bands observed at 279, 298, 327, 340, 406, 1135, 1241 cm^{-1} for FT-Raman spectra are assigned to a CF_3 symmetric stretching (1227 cm^{-1}), and two SO_2 antisymmetric stretching modes [19, 46-47]. The strong bands at 1137, 1184 for FT-IR spectra are associated to the trans-form vibrations [47]. The very strong Raman band and the shoulder observed in the region below 200 cm^{-1} are associated to a cation-anion interaction and intramolecular normal modes [49].

3.8.Thermal analysis:

Generally, ionic liquids are stable chemically and thermally, these advantages are directly linked to their applications in several industrial processes [50]; therefore, the knowledge of the thermal stability of ILs provides valuable information on their application domain [4,17, 29]. The thermal stabilities of three studied [C_{10}DABCO]-based ionic liquids were investigated using the thermogravimetric analysis (TGA) method. TGA thermograms are illustrated in **Figure 8**.

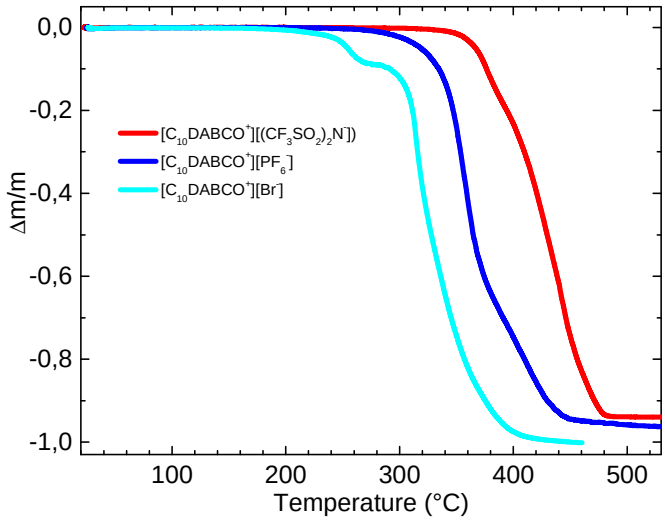

Figure 8: Thermogravimetric analysis (TGA) thermograms for synthesized [C_{10}DABCO][X](with X = $[Br]^-$,$[PF_6]^-$and $[N(SO_2CF_3)_2]^-$).

Upon heating, the TGA curves of [$C_{10}DABCO^+$] ILs show that their decomposition start at 220-240°C and in the temperature range 350–480 °C the complete decomposition occurs, depending on their structures and especially their coupled anion type [42-43, 50]. Thus from these curves and depending on [$C_{10}DABCO^+$] IL ionic liquid type, it can be safely interpreted that the thermal stability follow the order: [C_{10}DABCO][Br] < [C_{10}DABCO][PF_6] < ([C_{10}DABCO][$N(SO_2CF_3)_2$]) , which indicated that $[N(SO_2CF_3)_2]^-$ is thermodynamically more stable [29, 42]. Compared with fluorinated anions $[PF_6]^-$ and $[N(SO_2CF_3)_2]^-$, it is clear that [C_{10}DABCO][Br] significantly reduce thermal stability since they possess both a relatively high nucleophilic and basic character [44, 50]. Moreover, a larger size of $[N(SO_2CF_3)_2]^-$ anion tended to induce thermal decomposition of [C_{10}DABCO][$N(SO_2CF_3)_2$] IL at a higher temperature. In addition, it was also indicated that investigated IL exhibited the best thermal stability compared with analogue bromide due to the strong ionic linkage

between the cation $[C_{10}DABCO]^+$ and the anion $[N(SO_2CF_3)_2]^-$ and the anion's inability to hydrogen bond. To the best of our knowledge, there are no other reports of the thermal stability of these three selected ILs.

Conclusion

In the first experimental step, three ionic liquids based (ILs) on the 1-decyl-1,4-diazabicyclo [2.2.2] octane (DABCO) cation were synthesized. As anions $[Br]^-$, $[PF_6]^-$ and $[N(SO_2CF_3)_2]^-$ were selected. The structure of the obtained ILs were confirmed by ^1H, ^{13}C,^{19}F and ^{31}P-NMR spectroscopy and characterized by infrared and Raman spectroscopies. The thermal behavior confirmed that $[C_{10}DABCO]$ ILscontaining $[N(SO_2CF_3)_2]^-$ and $[PF_6]^-$ are more stable that the bromide $[Br]^-$,and they show a good thermal stability up to 360°C which makes them suitable for thermal application. In the next theoretical step, the electrostatic potential (ESP) maps, structural parameters, interaction energies, are studied and analyzed by means of DFT calculations at the M06-2X-GD3/AUG–cc–pVDZ level of theory. The result indicated that the contribution of dispersion energies obtained by using M06-2X-D3 functional for $[C_{10}DABCO][N(SO_2CF_3)_2]$ (s$\parallel$), $[C_{10}DABCO][N(SO_2CF_3)_2]$ (s$\perp$), $[C_{10}DABCO][N(SO_2CF_3)_2]$ (as$\parallel$) and $[C_{10}DABCO][N(SO_2CF_3)_2]$ (as$\perp$) ILs are higher than for $[C_{10}DABCO][Br]$ and $[C_{10}DABCO][PF_6]$ ILs. Also, the non-covalent interaction (NCI) and atoms in molecule (AIM) analysis results confirm the existence of non-covalent interactions such as van der Waals (vdW) interactions and weak hydrogen bond interactions between the cation and the anions and also steric repulsion in rings of the three studied ILs. In addition, natural bond orbital (NBO) and frontier molecular orbital (FMO) analysis results indicated that the transferred charge decreases on going from $[Br]^-$ anion to $[PF_6]^-$ one as the interaction energy decreases. Finaly, by using Electrochemical window (ECW) analysis, it is predicted that $[C_{10}DABCO][Br]$ and $[C_{10}DABCO][PF_6]$ ILs with the ECW about 5.48 V have more electrochemical stability than $[C_{10}DABCO][N(SO_2CF_3)_2]$ (s$\parallel$) IL for use in electrochemical devices.

Acknowledgements. This work was supported by The Ministry of Higher Education and Scientific Research (MESRS) of Algeria in PRFU project code: B00L01UN200120180002.

Supporting Information Available: Figure S1, Tables S1-S2.

Conflicts of interest

All authors declare that there are no conflicts of interest.

References

[1] K.Ślusarczyk, M.Flejszar, P. Chmielarz, From non-conventional ideas to multifunctional solvents inspired by green chemistry: fancy or sustainable macromolecular chemistry? Green Chem.25(2) (2023)522-42, https://doi.org/10.1039/D2GC03558H.

[2] J. L.Shamshina, R. D. Rogers, Commercialization of Ionic Liquids in Pursuit of Green Chemistry: Must we Each Become an Entrepreneur? Chem. Rec.23(8)(2023) e202200256, https://doi.org/10.1002/tcr.202200256.

[3] J.Song, Research progress of ionic liquids as lubricants. ACS Omega 6(44) (2021) 29345-29349, https://doi.org/10.1021/acsomega.1c04512.

[4]E. Fabre, S. S. Murshed, A review of the thermophysical properties and potential of ionic liquids for thermal applications, J. Mater. Chem.A 9(29) (2021) 15861-15879, https://doi.org/10.1039/D1TA03656D.

[5]M. M.Seitkalieva, D. E.Samoylenko, K. A.Lotsman, K. S.Rodygin, V. P. Ananikov, Metal nanoparticles in ionic liquids: Synthesis and catalytic applications,Coord. Chem. Rev.445 (2021) 213982, https://doi.org/10.1016/j.ccr.2021.213982.

[6]B.Haddad, D.Villemin, E. H. Belarbi, Synthesis of palladium-bidentate complex and its application in Sonogashira and Suzuki coupling reactions. Chem. Pap.68 (2014) 656-661, https://doi.org/10.2478/s11696-013-0489-3.

[7]B.Fetouhi, B.Haddad, S. A.Brandán, A.Paolone, D.Villemin,M.Boumediene, M. Rahmouni, S.Bresson, Synthesis, molecular structure, and properties of DABCO bromide based ionic liquid combining spectroscopic studies with DFT calculations, J. Mol. Struct. 1233,(2021) 130102, https://doi.org/10.1016/j.molstruc.2021.130102.

[8] M. J.Aalam, Deepa, P. Chaudhary, D. R.Meena, G. D. Yadav, S.Singh, DABCO-based chiral ionic liquids as recoverable and reusable organocatalyst for asymmetric Diels–Alder reaction. Chirality 34(1) (2022) 134-146, https://doi.org/10.1002/chir.23385.

[9] G. D. Yadav, Deepa, & S. Singh, 1, 4-Diazabicyclo [2.2. 2] octane trifluoroacetate: A highly efficient organocatalyst for the cyanosilylation of carbonyl compounds under solvent free condition. *ChemistrySelect*, *2*(17) (2017) 4830-4835.
https://doi.org/10.1002/slct.201700674

[10] G. D. Yadav, M. J. Aalam, P. Chaudhary, , & S. Singh, Synthesis of Dihydropyrimidinones (DHPMs) and Hexahydro Xanthene Catalyzed by 1, 4-Diazabicyclo [2.2. 2] Octane Triflate Under Solvent-Free Condition. *Current Organic Synthesis*, *16*(5), (2019) 776-786.
https:// 10.2174/1570179415666181113154232.

[11] A. Wykes, S. L. MacNeil, Synthesis of New lewis basic room-temperature ionic liquids by monoquaternization of 1, 4-diazabicyclo [2.2. 2] octane (DABCO), Synlett 2007(01), (2007) 0107-0110, https://doi.org/10.1055/s-2006-956460.

[12]M. Faisal,A.Haider, , Q.ulAein, A.Saeed, F. A. Larik, Deep eutectic ionic liquids based on DABCO-derived quaternary ammonium salts: A promising reaction medium in gaining access to terpyridines. Front.chem. Sci. Eng. 13 (2019) 586-598, https://doi.org/10.1007/s11705-018-1788-6.

[13] P.Mondal, S. Chatterjee, P.Sarkar, A.Bhaumik, C.Mukhopadhyay, Preparation of DABCO-Based Acidic-Ionic-Liquid-Supported ZnO Nanoparticles and Their Application for Ecofriendly Synthesis of N-Aryl PolyhydroquinolineDerivatives,ChemistrySelect, 4(40) (2019) 11701-11710, https://doi.org/10.1002/slct.201902427.

[14] A. Ying, Z.Li, J.Yang, S.Liu, S.Xu, H.Yan, C.Wu, DABCO-based ionic liquids: recyclable catalysts for aza-Michael addition of α, β-unsaturated amides under solvent-free conditions, J. Org. Chem.79(14) (2014) 6510-6516, https://doi.org/10.1021/jo500937a.

[15]J.Zhang, R.Liu, X.Liu, J.Li, R.Wu, Y.Yang, Study on extraction of Rh (III) by DABCO-based ionic liquid from hydrochloric acid medium, Sep. Purif. Technol.324(2023)124578, https://doi.org/10.1016/j.seppur.2023.124578.

[16] M.Ishtiaq, M. A.Khan, S. Ahmed, S.Ali,M.Al-Rashida, S.Iftikhar, S.TariqueMoin, A. Hameed, Probing new DABCO-F based ionic liquids as catalyst in organic synthesis. J. Mol. Struct.1268(2022) 133638, https://doi.org/10.1016/j.molstruc.2022.133638.

[17]B. Haddad, S. A. Brandán, B. Fetouhi, M. Boumediene, A. Paolone, D. Villemin, M. Rahmouni, S. Bresson, Synthesis, NMR, vibrational spectroscopy, thermal and DFT studies of new DABCO hexafluorophosphate based ionic liquid. J. Mol.Struct. 1258 (2022)132682, https://doi.org/10.1016/j.molstruc.2022.132682.
[18]Y.Lauw, T.Rüther, M. D.Horne, K. S.Wallwork, B. W.Skelton, I. C.Madsen, T.Rodopoulos, Structural studies on the basic ionic liquid 1-ethyl-1, 4-diazabicyclo [2.2. 2] octaniumbis (trifluoromethylsulfonyl) imide and its bromide precursor. Cryst. Growth Des. 12(6)(2012) 2803-2813,https://doi.org/10.1021/cg201592u.
[19]B. Haddad, S. A. Brandán, B. Fetouhi, A. Paolone, M. Boumediene, D. Villemin, M, Rahmouni, S. Bresson, Synthesis, NMR, IR, Raman spectra and DFT calculations of 1-octyl-1, 4-diazabicyclo [2.2. 2] octan-1-ium bis (trifluoromethylsulfonyl) imide, J. Mol. Struct.1288 (2023)135792, https://doi.org/10.1016/j.molstruc.2023.135792.
[20] N. Jamasbi, M. Irankhah-Khanghah, F. Shirini, H. Tajik, M.S.N. Langarudi, DABCO-based ionic liquids: introduction of two metal-free catalysts for one- pot synthesis of 1, 2, 4-triazolo [4, 3-a] pyrimidines and pyrido [2, 3-d] pyrim- idines, NJC 42 (11) (2018) 9016–9027, https://doi.org/10.1039/C8NJ01455H .
[21] B.Khalili, M.Rimaz, An investigation on the physicochemical properties of the nanostructured [(4-X) PMAT][N (CN)2] ion pairs as energetic and tunable aryl alkyl amino tetrazolium based ionic liquids, J. Mol. Struct. 1137 (2017) 530-42, https://doi.org/10.1016/j.molstruc.2017.02.053.
[22] B. Khalili, M. Rasoulian, K. Ghauri, First time investigation of the substitution effect at anion part of the ILs on their physicochemical properties using [DMT][4-XPhSO3](X= NH2, OH, H, F, Br, CHO, CF3, CN and NO2) as a model ILs: A systematic DFT study, J. Mol. Struct. 1201 (2020) 127171, https://doi.org/10.1016/j.molstruc.2019.127171.
[23] B. Khalili, M. Moosavi, K. Ghauri, New task-specific ionic liquids based on phenyl diazenyl methyl pyridinium cation: Energetic, electronic and optical properties exploration based on DFT calculations, J. Mol. Graph. Model.118 (2023) 108352, https://doi.org/10.1016/j.jmgm.2022.108352.
[24] B. Khalili, M. Moradpour, Fluorination effects on the physicochemical properties of the nanostructured tunable ionic liquids:[5F-PhMeTAZ]+ or [5H-PhMeTAZ]+ which one is the better choice?J. Fluor. Chem. 257–258 (2022) 109970, https://doi.org/10.1016/j.jfluchem.2022.109970.
[25] B.Khalili M. Pour Amani, K. Ghauri, Exploring of spacer fluorination effect on the characteristics and physicochemical properties of the newly designed task specific dicationicimidazolium-based ionic liquids: A quantum chemical approach, J. Fluor. Chem. 261–262 (2022) 110026, https://doi.org/10.1016/j.jfluchem.2022.110026.
[26] B. Khalili · S. Heydari· K. Ghauri, Dicationic ionic liquids (DILs) based on the phenyl and perfluoro-phenyl π-spacer-linked triazolium cations: a quantum chemical comparative study, Theor. Chem. Acc. 141 (2022) 67, https://doi.org/10.1007/s00214-022-02931-4.
[27] B. Khalili, M. Rimaz, Does interaction between an amino acid anion and methylimidazolium cation lead to a nanostructured ion pairs of [Mim][AA] as an ionic liquid? J. Mol. Liq. 229 (2017) 267, https://doi.org/10.1016/j.molliq.2016.12.077.
[28] B. Khalili, M. Mamaghani, N. Bazdid-Vahdati, Structural design and physicochemical specifications exploring of the new di-cationic ionic liquids (D-ILs) composed of para-xylyl linked N-Methylimidazolium cation and various anions: a full M06–2X computational study, Theor. Chem. Acc. 141(1) (2022)1, https://doi.org/10.1007/s00214-021-02862-6.
[29] B. Haddad, M. Boumediene, B. Khalili, K. Ghauri, A. Paolone, S. Taibi, W. Yazid, M. A. Assenine, D. Villemin, M. Rahmouni, S. Bresson, Synthesis, vibrational and thermal studies of new 3, 3′-dibutyl-1, 1′-(1, 4-phenylenedimethylene)-bis (1H-imidazolium) ionic liquids: An experimental and quantum computational investigation, J. Mol. Struct. 1300 (2024) 137325, https://doi.org/10.1016/j.molstruc.2023.137325.
[30] A. Singh, P. Singh, N. Goel, Theoretical study of DABCO-based ionic liquid: synthesis and reaction mechanism, Struct. Chem. (2014) 821-8, https://doi.org/10.1007/s11224-013-0348-4.
[31] S. Grimme, S. Ehrlich, L. Goerigk, Effect of the dampingfunction in dispersion corrected density functional theory, J. Comput. Chem. 32 (2011) 1456–1465,https://doi.org/10.1002/jcc.21759.
[32] A. Mohajeri, A. Ashrafi, Structure and ElectronicProperties of Amino Acid IonicLiquids. J. Phys. Chem. A 115 (2010) 6589−6593, https://doi.org/10.1021/jp1093965.

[33] P. A. Hunt, I. R. Gould, B. Kirchner, The Structure of Imidazolium-Based Ionic Liquids: Insights From Ion-Pair Interactions, Aust. J. Chem. 60 (2007) 9−14, https://doi.org/10.1071/CH06301.
[34] H. Roohi, S. F. Gildeh, M. Mehrdad, K. Ghauri, Exploring the physicochemical properties of para-xylyl linked DBU-based dicationic ionic liquids consist of various anions: a GD3–M06–2X study,J. Mol. Liq. 310 (2020) 113060, https://doi.org/10.1016/j.molliq.2020.113060.
[35] W. Wu, Y. Lu, Y. Liu, H. Li, C. Peng, H. Liu, W. Zhu, Structures and electronic properties of transition metal-containing ionic liquids: Insights from ion pairs, J. Phys. Chem. A 118 (13) (2014) 2508-18, https://doi.org/10.1021/jp4125167.
[36] A. Bayat, A. Fattahi, Influence of remote intramolecular hydrogen bonding on the acidity of hydroxy-1, 4-benzoquinonederivatives: A DFT study, J. Phys. Org. Chem.32(4) (2019) 3919, https://doi.org/10.1002/poc.3919.
[37] S. P. Ong, G. Ceder Investigation of the effect of functional group substitutions on the gas-phase electron affinities and ionization energies of room-temperature ionic liquids ions using density functional theory, ElectrochimicaActa 55(11) (2010) 3804-11, https://doi.org/10.1016/j.electacta.2010.01.091.
[38] Haddad, B., Pandey, D. K., Singh, D. K., Paolone, A., Drai, M., Villemin, D., & Bresson, S. (2023). Effect of isopropyl side chain branching and different anions on electronic structure, vibrational spectra, and hydrogen bonding of isopropyl-imidazolium-based ionic liquids: Experimental and theoretical investigations. *Spectrochimica Acta Part A: Molecular and Biomolecular Spectroscopy*, 122325. https://www.sciencedirect.com/science/article/abs/pii/S1386142523000100
[39] M.A. Assenine, B. Haddad, A. Paolone, S.A. Brandán, D. Villemin, M. Boumediene, M. Rahmouni, S. Bresson, Experimental and DFT studies on structure, spectroscopic and thermal properties of N-Methyl-N,N,N-trioctylammonium chloride ionic liquid, Journal of Molecular Structure 1230 (2021).
https://doi.org/10.1016/j.molstruc.2020.129625
[40] M.A. Assenine, B. Haddad, A. Paolone, S.A. Brandán, M. Goussem, D. Villemin, M. Boumediene, M. Rahmouni, S. Bresson, Synthesis, thermal properties, vibrational spectra and computational studies of Trioctylmethylammonium bis(trifluoromethylsulfonyl)imide ionic liquid, Journal of Molecular Structure 1232 (2021). https://doi.org/10.1016/j.molstruc.2021.130085
[41] B. Haddad, S.A. Brandán, M.A. Assenine, A. Paolone, D. Villemin, S. Bresson, Bidentate cation-anion coordination in the ionic liquid 1-ethyl-3-methylimidazolium hexafluorophosphate supported by vibrational spectra and NBO, AIM and SQMFF calculations, Journal of Molecular Structure 1212 (2020).
https://www.sciencedirect.com/science/article/abs/pii/S0022286020304294
[42] Boumediene, M., Haddad, B., Paolone, A., Assenine, M. A., Villemin, D., Rahmouni, M., & Bresson, S. (2020). Synthesis, conformational studies, vibrational spectra and thermal properties, of new 1, 4-(phenylenebis (methylene) bis (methyl-imidazolium) ionic liquids. *Journal of Molecular Structure*, *1220*, 128731.
https://www.sciencedirect.com/science/article/abs/pii/S0022286020310565
[43] Boumediene, M., Haddad, B., Paolone, A., Drai, M., Villemin, D., Rahmouni, M., ... & Abbas, O. (2019). Synthesis, thermal stability, vibrational spectra and conformational studies of novel dicationic meta-xylyl linked bis-1-methylimidazolium ionic liquids. *Journal of Molecular Structure*. 1186, 68-79.
https://doi.org/10.1016/j.molstruc.2019.03.019
[44] D. Hadji, B. Haddad, S.A. Brandán, S.K. Panja, A. Paolone, M. Drai, D. Villemin, S. Bresson, M. Rahmouni, Synthesis, NMR, Raman, thermal and nonlinear optical properties of dicationic ionic liquids from experimental and theoretical studies, Journal of Molecular Structure 1220 (2020).
https://doi.org/10.1016/j.molstruc.2020.128713
[45] E.R. Talaty, S. Raja, V.J. Storhaug, A. D€olle, W.R. Carper, Raman and infraredspectra and ab initio calculations of C2-4MIM imidazoliumhexafluorophosphateionic liquids, J. Phys. Chem. B 108 (35) (2004) 13177-13184, https://doi.org/10.1021/jp040199s.
[46]B.Haddad, A.Paolone,D.Villemin, M.Taqiyeddine, E. H.Belarbi, S.Bresson, M. Rahmouni, N.R. Dhumal, H.J. Kim, J.Kiefer, Synthesis, conductivity, and vibrational spectroscopy of

tetraphenylphosphonium bis (trifluoromethanesulfonyl) imide. J. Mol. Struct.1146 (2017) 203-212, https://doi.org/10.1016/j.molstruc.2017.05.138.
[47] M.Drai, A.Mostefai, A.Paolone, B. Haddad, E.Belarbi, D.Villemin, M. Rahmouni, Synthesis, experimental and theoretical vibrational studies of 1-methyl and 1, 2-dimethyl, 3-propyl imidazoliumbis (trifluoromethanesulfonyl) imide. *Journal of Chemical Sciences*, 129(6) (2017) 707-719, https://doi.org/10.1007/s12039-017-1282-6.
[48]B.Haddad, A.Paolone,D.Villemin, J. F.Lohier, M.Drai, S.Bresson, E. H. Belarbi, para-Xylyl bis-1-methylimidazolium bis (trifluoromethanesulfonyl) imide: Synthesis, crystal structure, thermal stability, vibrational studies. J. Mol. Liq.260 (2018) 391-402,https://doi.org/10.1016/j.molliq.2018.03.113.
[49]Haddad, B., Mokhtar, D., Goussem, M., Belarbi, E. H., Villemin, D., Bresson, S., ... & Kiefer, J. (2017). Influence of methyl and propyl groups on the vibrational spectra of two imidazolium ionic liquids and their non-ionic precursors. *Journal of Molecular Structure*, *1134*, 582-590. https://doi.org/10.1016/j.molstruc.2017.01.008
[50]A.Paolone,B. Haddad,D.Villemin, M.Boumediene,B.Fetouhi, M. A. Assenine, Thermal Decomposition, Low Temperature Phase Transitions and Vapor Pressure of Less Common Ionic Liquids Based on the Bis (trifuoromethanesulfonyl) imide Anion. Mater.15(15) (2022) 5255, https://doi.org/10.3390/ma15155255.